Bull. Mater. Sci. (2018) 41:4
https://doi.org/10.1007/s12034-017-1538-2

Adsorption property of volatile molecules on ZnO nanowires: computational and experimental approach

A NANCY ANNA ANASTHASIYA[1], S RAMYA[1], D BALAMURUGAN[1], P K RAI[2] and B G JEYAPRAKASH[1,*]

[1]Functional Nanomaterials Lab, Centre for Nanotechnology and Advanced Biomaterials (CeNTAB), School of Electrical and Electronics Engineering, SASTRA University, Thanjavur 613401, India

[2]Centre for Fire Explosive and Environment Safety, Defence Research and Development Organisation, Ministry of Defence, Timarpur, Delhi 110054, India

*Author for correspondence (jp@ece.sastra.edu)

MS received 14 March 2017; accepted 26 April 2017; published online 2 February 2018

Abstract. ZnO nanowires (NWs) were deposited on a glass substrate by the successive ionic layer adsorption and reaction method (SILAR). Sensing response of ZnO NWs towards reducing vapours was tested at ambient temperature (∼32°C) by the chemiresistor method. The vapour response was found to be 80.2, 1.6, 1.1 and 1.1 for NH_3, H_2O, $(CH_3)_2CO$ and C_2H_5OH, respectively. Also, density functional theory (DFT) calculations were performed to understand the charge transfer and electronic property change during adsorption of molecules over ZnO NW. The band of the Zn 3d state was altered after adsorption and no significant changes were observed in the O 2p state. Higher binding energy (14.6 eV) with significant charge transfer ($0.04|e|$) was observed in the ammonia-adsorbed ZnO NW. On comparing response obtained through experimental and computational studies, almost a similar trend of response was observed except for the H_2O–ZnO system. This was due to lack of dispersion interaction and steric effect influence in the DFT calculation with the chosen computational methods.

Keywords. ZnO; interaction; ammonia; band structure; density of states.

1. Introduction

As far as the chemical sensing properties are concerned, ZnO is promising and the most widely used candidate for gas/vapour-sensing materials; n-type ZnO was used as a sensing element for HCHO [1], CO [2], CO_2 [3], SF_6 [4], NO_2 [5], H_2S [6], H_2 [7], NH_3 [8], C_2H_6O [9] and humidity [10]. Along with the experimental research, many researchers are working on the understanding of the atomistic interaction of gases with ZnO surface. Martins *et al* [11] studied the interaction of H_2, CO, CO_2, H_2O and NH_3 on ZnO $(10\bar{1}0)$ surface using cluster model in Gaussian 03 package [11]. The charge distribution, binding energy and orbital energies were considered for the adsorption studies and the obtained results were compared with the available experimental results. Prades *et al* [12] reported that Zn surface atom is the preferred site for NO_2 adsorption rather than SO_2. Also, the temperature-dependent stoichiometric stability was studied and adsorption of target molecules was analysed. CO adsorption on the polar and nonpolar ZnO surface was studied through density functional theory (DFT) approach by Meyer and Marx [13]. Effect of CO orientation and hydrogen coverage on the polar ZnO surface was reported. Their finding reveals that the Zn ion is the binding site for CO adsorption. After hydrogen saturation, the OH-terminated $(000\bar{1})$ surface was found to be favourable [13]. In general, the gas sensing mechanism is understood based on vacant oxygen ion and direct adsorption method. However, adsorption sites and the kind of interaction mecahnism are not yet understood completely.

The metal oxide surface consists of unsaturated oxygen and metal ions, which act as Lewis base and Lewis acid sites, respectively. Noei *et al* [14] studied the adsorption of NH_3 on ZnO by high-resolution electron energy loss spectroscopy (HREELS), thermal desorption spectroscopy (TDS) and theoretical calculations. These findings reveal that the lone pair of electrons in the N atom coordinates to Zn^{2+} ion [14–16]. The hydrogen, ammonia, carbon monoxide and ethanol adsorptions over the $(10\bar{1}0)$ ZnO surface were studied by Yuan *et al* [17] by considering the Zn site as an adsorption site. In the present work, Zn site was chosen as an adsorption site for a theoretical calculation. As mentioned earlier, various gases and vapours were detected by ZnO nanostructures. Among these many nanostructures, nanowires (NWs) have unique properties due to the higher aspect ratio and better charge transport. ZnO NWs were prepared and moulded for the experimental and theoretical analysis of gas–solid interaction.

The present work focuses on the interaction of reducing molecules with n-type ZnO by both experimental and theoretical studies. For the experimental studies, the reducing vapours were used as a source. The chosen molecules were ethanol, acetone, ammonia and water due to the need for detection in diverse areas.

2. Computational and experimental details

Virtual NanoLab [18] software was utilized to construct the ZnO NWs with 24 Zn atoms and 24 O atoms. DFT calculations were performed with the Quantum Wise Atomistix Toolkit (ATK) package [19,20]. For exchange correlation the Perdew–Burke–Ernzerhof (PBE) [21] parameterized generalized gradient approximation (GGA) was applied for the electronic structural studies. The K-point was sampled as a $5 \times 5 \times 5$ unit and charge transfer studies were made using Mulliken population analysis [22]. The binding energy was estimated as follows:

$$E_{\mathrm{b}} = E_{\text{adsorbed ZnO}} - (E_{\text{molecule}} + E_{\text{ZnO}}), \tag{1}$$

where E_{b}, $E_{\text{adsorbed ZnO}}$, E_{molecule} and E_{ZnO} are the binding energy, the total energy of the ZnO NW system after adsorption, the total energy of the molecule and total energy of the ZnO NW, respectively. The response of the ZnO NWs is governed by band gap [17] and given as follows:

$$S = \frac{R_0}{R_{\mathrm{v}}} = \exp\left(\frac{E_0 - E_{\mathrm{m}}}{k_{\mathrm{B}}T}\right), \tag{2}$$

where S is a response, k_{B} is the Boltzmann constant (8.617×10^{-5} eV K^{-1}), T is operating temperature (300 K), E_0 is the band gap of bare ZnO NWs and E_{m} is the band gap of reducing-molecule-adsorbed ZnO NW.

ZnO NWs were deposited on a glass substrate using a HO-TH-03D successive ionic layer adsorption and reaction (SILAR) instrument (HOLMARC make); 0.1 M of zinc sulphate solution [23] and boiling deionized water were used as cationic and anionic solution, respectively. The deposition cycles and dip duration were 150 cycles and 5 s, respectively. The prepared ZnO thin film was characterized by

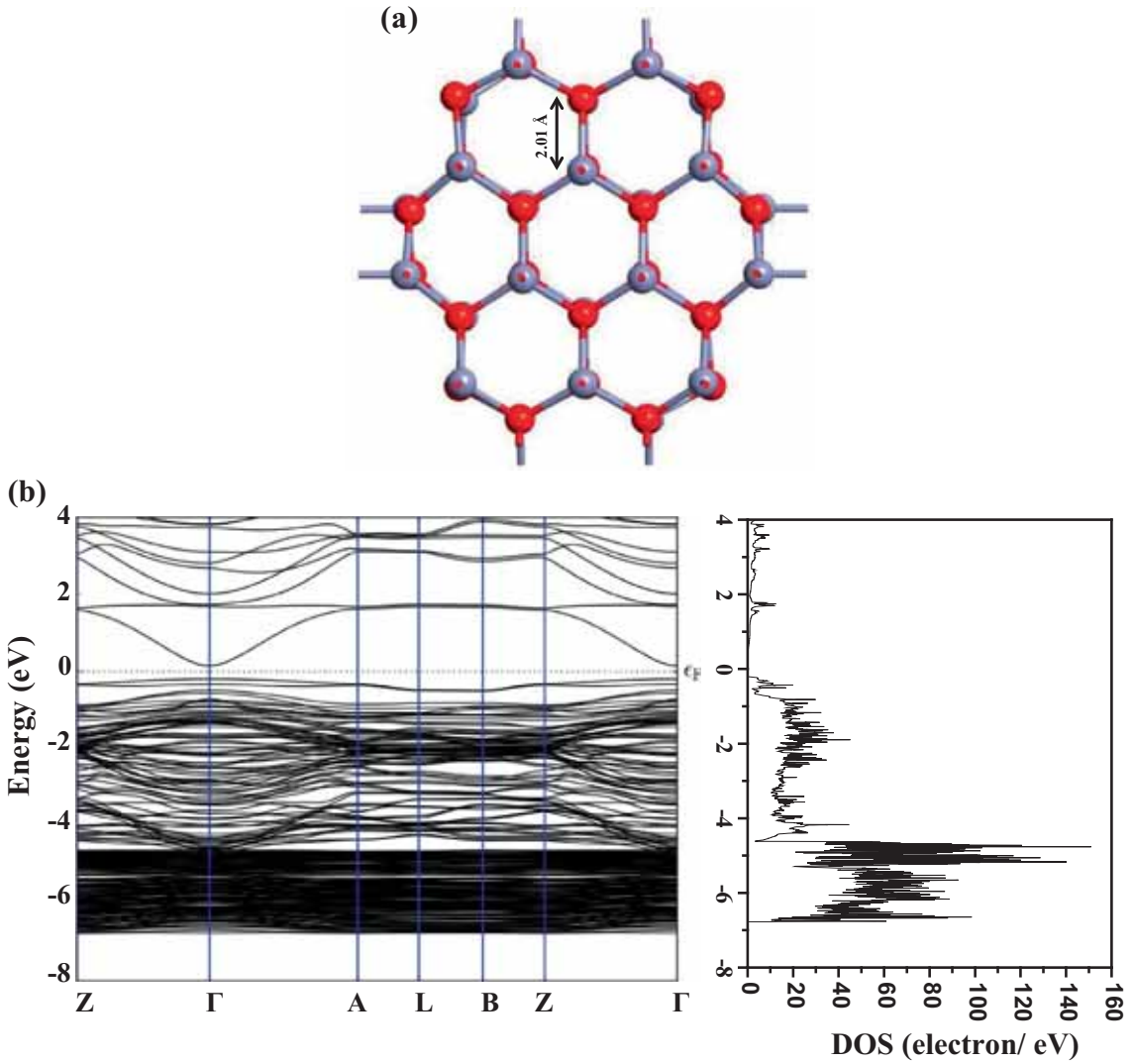

Figure 1. (**a**) Optimized structure of the ZnO nanowire system. (**b**) Band structure and density of state of the ZnO nanowire.

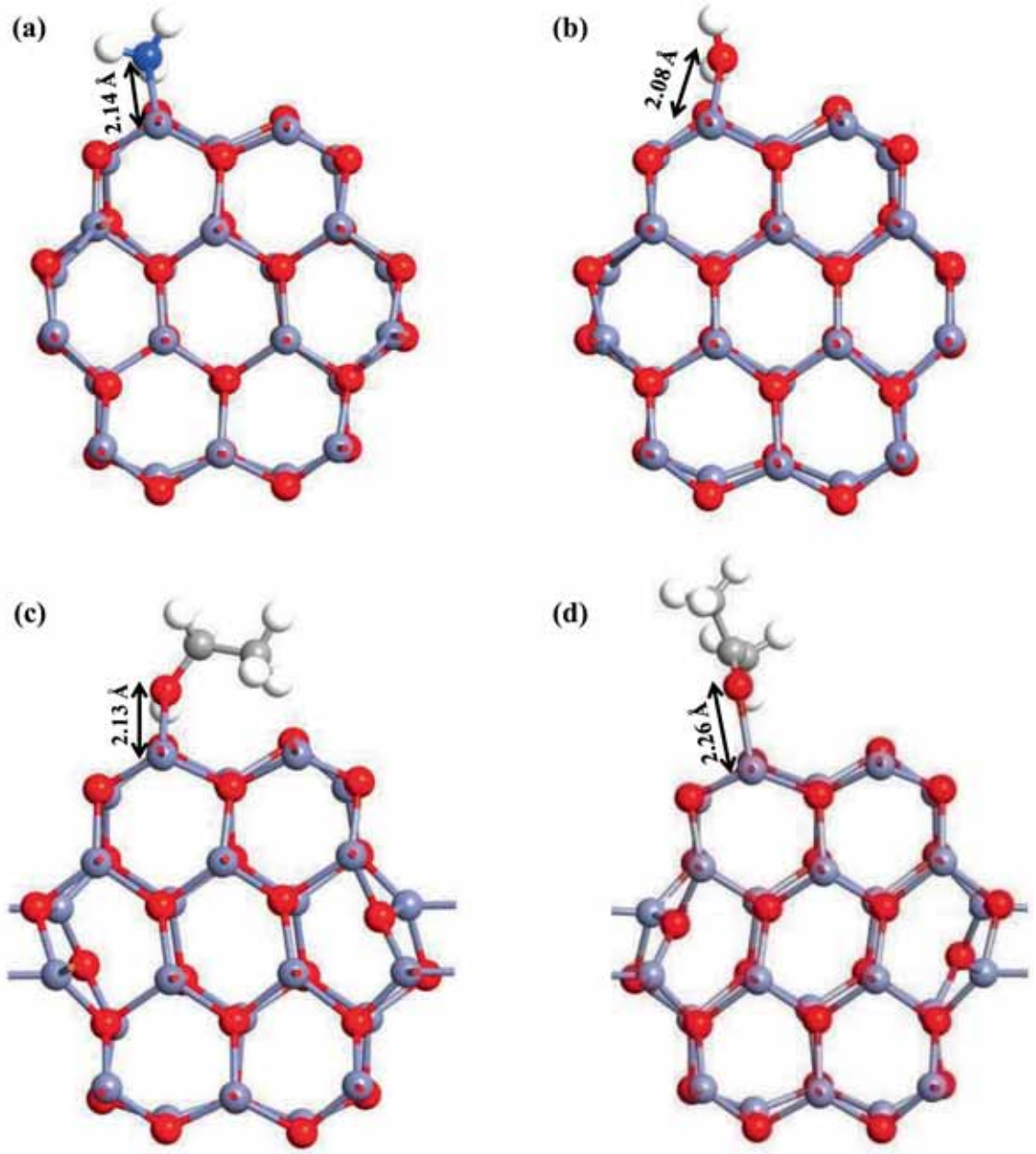

Figure 2. Optimized structure of the ZnO NW after the adsorption of (**a**) NH_3, (**b**) H_2O, (**c**) C_2H_5OH and (**d**) $(CH_3)_2CO$ molecules.

field-emission scanning electron microscopy (FESEM) and X′ PERT PRO PANalytical X-ray diffractometry (XRD). The electrical contact was made using silver epoxy and thin copper wire. The dimension of the sensing element was 1 × 1 cm^2 and the applied voltage during the detection was 9 V DC. The current changes were recorded for 2 s once using an Ivium Vertx DC electrometer. The sensing studies were carried out using a home-built gas sensor testing set-up [24]. The sensor was operated at ambient temperature (32°C) and the relative humidity of 65% RH.

3. Results and discussion

3.1 *Theoretical studies*

Figure 1a shows a side view of ZnO NW and electronic structure (band structure and density of state) of the ZnO NW system is presented in figure 1b. The bond length between the Zn and O in the ZnO NW is 2.01 Å. The ZnO NW has a direct band gap with a value of 0.34 eV at Γ point in the reciprocal space. The valence band (VB) and conduction band (CB) edges for the ZnO NW are located at −0.204 and 0.138 eV,

Table 1. VB edge, CB edge, band gap, binding energy, charge transfer and response values of bare and adsorbed molecules ZnO NW systems.

System	VB edge (eV)	CB edge (eV)	Band gap (eV)	Binding energy (eV)	Charge transfer (electrons)	Response
ZnO nanowire	−0.204	0.138	0.342			
NH_3/–ZnO	−0.157	0.101	0.258	14.6	0.04	25.3
H_2O/–ZnO	−0.218	0.012	0.230	11.3	0.08	76.0
$(CH_3)_2CO$/–ZnO	−0.182	0.120	0.302	12.8	0.02	4.7
C_2H_5OH/–ZnO	−0.448	0.33	0.778	3.2	−0.04	0

respectively. This value is smaller than the theoretical value of the bulk ZnO (0.73 eV) [25,26], which might be due to the diameter of the NW. Also, GGA level of theory within PBE gives an inaccurate description of ZnO band gap. It is due to spurious hybridization of Zn 3d bands with O 2p, which leads to underestimation of band gap [27]. The bottom of the VB around 17–18 eV arises due to the contribution of the O 2s state. The O 2p state and Zn 3d state are hybridized at the top of the VB. The major part of the O 2p state was located around −4 eV to the Fermi level and the Zn 3d state at −7 to −4 eV. The bottom of the CB was high due to the Zn 4s state.

Figure 2a, b, c and d shows a side view of ZnO NW after the adsorption of NH_3, H_2O, $(CH_3)_2CO$ and C_2H_5OH, respectively. After optimization, bond length between the bonded Zn with the adsorbed sites of NH_3, H_2O, $(CH_3)_2CO$ and C_2H_5OH were 2.14, 2.08, 2.26 and 2.13 Å, respectively. The adsorption of the reducing molecule leads to the reconstruction of the ZnO NWs (figure 2a–d). The corresponding changes in the VB edge, CB edge, band gap, binding energy, charge transfer and response are given in table 1. On comparing the total energy of the ZnO NW and adsorbed ZnO NW system, an increase in the total energy is observed after the adsorption of the reducing molecule. Fermi energy was decreased after the adsorption of the reducing molecules (NH_3, H_2O and $(CH_3)_2CO$) (Fermi level was set as 0 eV). This means that conductivity increased when the film surface was exposed to the reducing molecules. For C_2H_5OH the chemical potential was increased; it was unfavourable. Hence, the system was not considered for the discussion. The VB edge was increased for NH_3–ZnO and $(CH_3)_2CO$–ZnO systems, whereas it was decreased for H_2O–ZnO and C_2H_5OH–ZnO systems. The position of the CB edge was decreased after the adsorption of NH_3, H_2O and $(CH_3)_2CO$ molecules. Hence, the resultant band gap value was decreased after adsorption of the reducing molecules. The band gap value was found to be high for $(CH_3)_2CO$–ZnO system with lesser charge transfer value of $0.02|e|$. The binding energy was estimated using equation (1). Among these reducing molecules, NH_3 showed high binding energy (14.6 eV) with the ZnO NW. It was shown that the NH_3-adsorbed ZnO NW system was stable at ambient temperature. Hence, one can expect a moderate recovery in the ambient condition of the stoichiometric ZnO NW during NH_3 vapour detection. The charge transfer value for NH_3–ZnO system was $0.04|e|$. The maximum charge transfer was observed for H_2O–ZnO to be $0.08|e|$. It revealed that the ZnO NW was sensitive to the humidity [10].

The changes in the band structure and density of states are shown in figure 3a, b, c and d for NH_3-, H_2O-, C_2H_5OH- and $(CH_3)_2CO$-adsorbed ZnO NWs system, respectively. The band of the Zn 3d state was altered after adsorption and no significant changes were observed in the O 2p state.This might be due to the negative work function of the system and nucleophilic nature of the chosen molecule.

3.2 *Experimental studies*

The cross-sectional morphology of the SILAR-deposited ZnO NWs is shown in figure 4. It shows the formation of thin ZnO layer parallel to the plane of the glass substrate, followed by vertically grown NWs (shown in figure 4a). The length and diameter of the vertically grown ZnO NWs range from 2.6 to 5 μm and 106 to 148 nm, respectively. This vertically grown NW with an aspect ratio of 25–34 might be due to the formation of the initial seed layer, the higher growth rate of the (002) plane and the number of deposition cycles. The surface energy of the glass substrate and deposition temperature of the anionic solution will lead to the chemisorption of the zinc hydroxide ion as nuclei and the seed layer. The size of these formed nuclei will decide the diameter of the NWs, which depends on the concentration of the cationic solution. The boiling temperature of the anionic solution and rinsing time in it are the important factors to obtain appropriate standalone NWs. The tilted alignment of the wires was due to the surface roughness of the seed layer (marked with red circles in figure 4b). After a growth of certain critical height at a constant temperature, the wire started to bend due to its small diameter (marked with the green circle in figure 4b). The *c*-axis growth was also verified through the XRD pattern shown in figure 5. XRD analysis was made using Cu$K\alpha_1$ X-rays. The peaks were indexed as (100), (002) and (101) planes with respect to the standard ICDD card number 36-1451. The impurity peaks, non-stoichiometric zinc and other phases of ZnO were not observed.

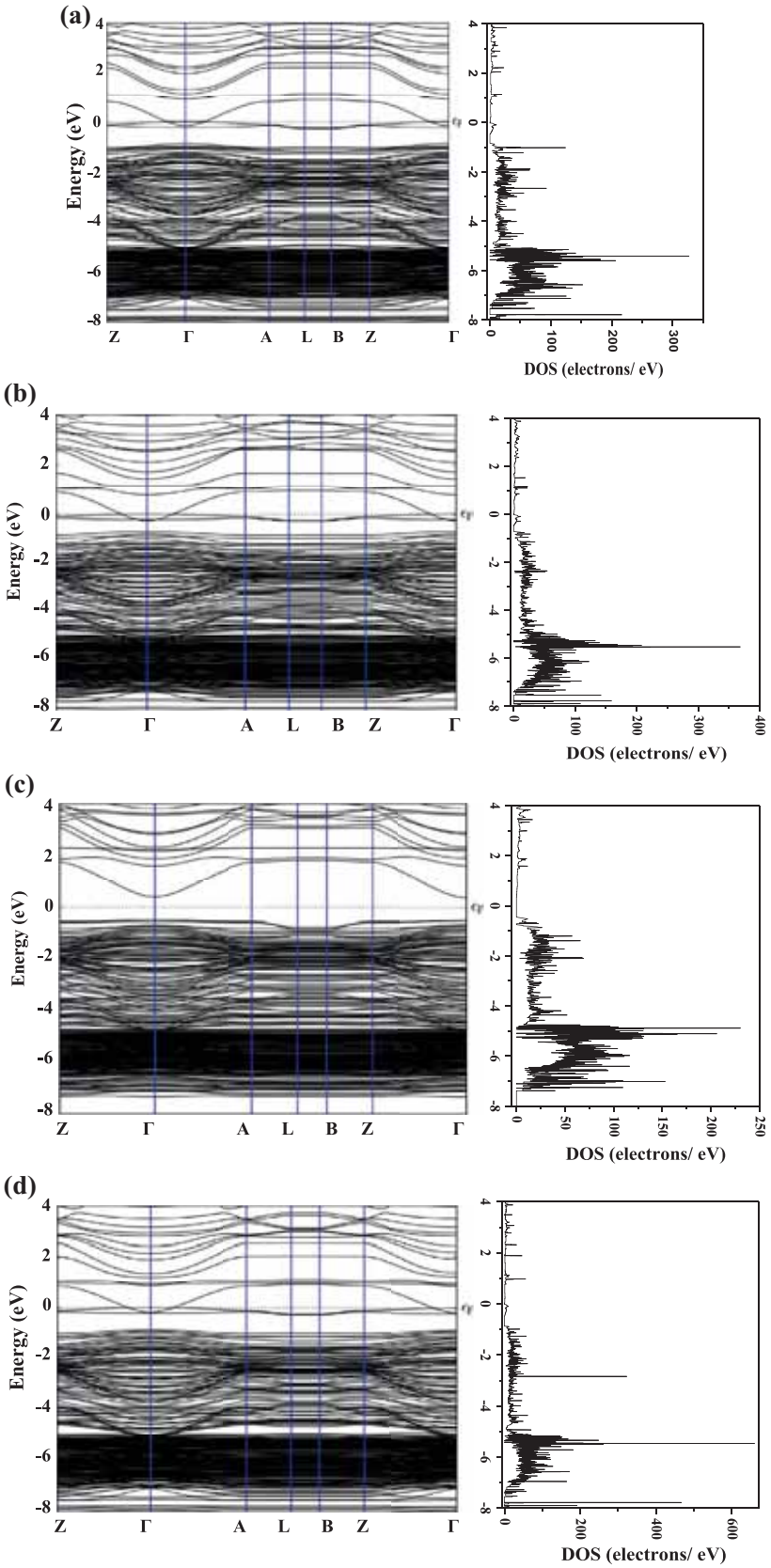

Figure 3. Electronic structure of the ZnO NW after adsorption of (**a**) NH_3, (**b**) H_2O, (**c**) C_2H_5OH and (**d**) $(CH_3)_2CO$ molecules.

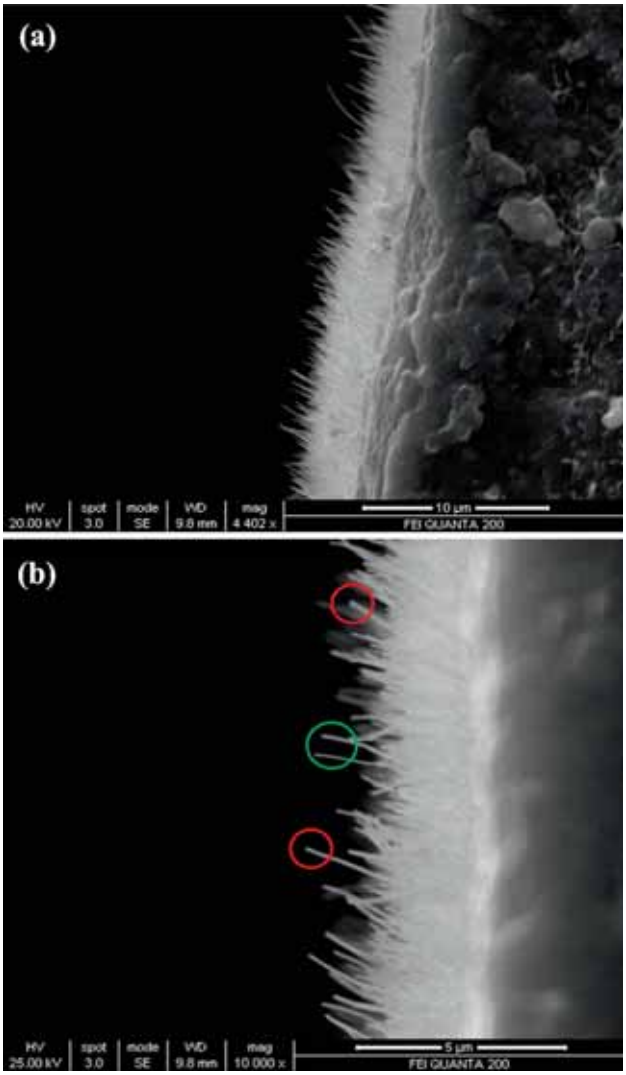

Figure 4. Cross-sectional scanning electron micrograph of the SILAR-deposited ZnO at (**a**) 4402× and (**b**) 10000× magnifications.

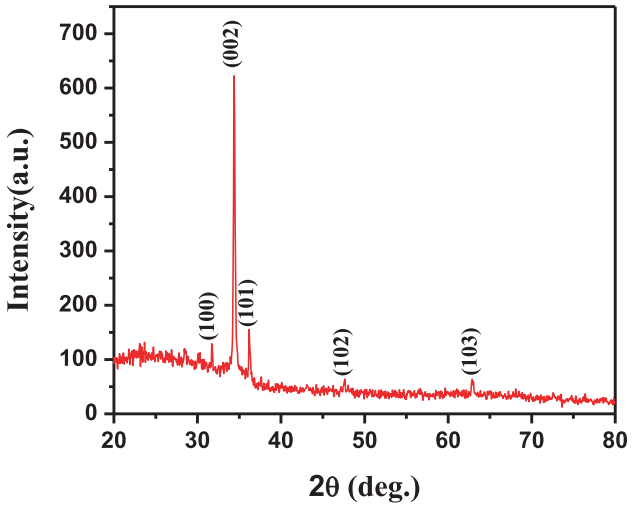

Figure 5. XRD pattern of as-deposited ZnO nanowires.

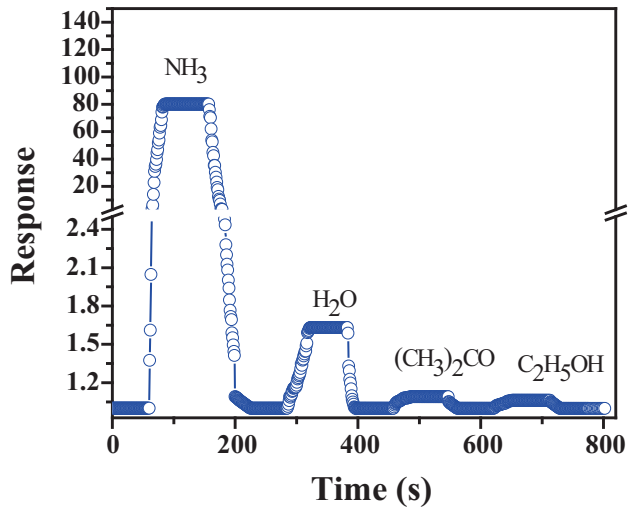

Figure 6. Transient response of ZnO NWs towards reducing vapours at 50 ppm.

3.3 *Sensing response of ZnO NWs*

The SILAR-deposited ZnO NWs were exposed to reducing vapour such as NH_3, H_2O, $(CH_3)_2CO$ and C_2H_5OH at ambient temperature (32°C). The required amount of the targeted liquid was injected into the home-built test chamber with the help of a chromatographic syringe to reach the desired concentration inside the chamber [24]. The vapour was evacuated using a vacuum pump. The electrical resistance of the ZnO NWs decreased for all the reducing vapours and the response was estimated using equation (2). Transient response of ZnO NW towards reducing vapours at 50 ppm is shown in figure 6. Sensing response of NH_3 was found to be high compared with the other reducing vapours. This is due to the lone pair of electrons present in the $3a_1$ state of NH_3 molecule [14] and energy level matching between Zn 3d and $NH_3 3a_1$ states [16]. Also, the kinetic diameter and ionization energy of ammonia were less than those of the other vapours [28]. The kinetic diameter refers to molecule size, which has an impact on sensing property of a material. The ammonia vapour with small kinetic diameter diffuses in the pore between ZnO NWs, which in turn leads to more adsorption sites and higher response. Also, ammonia has moderate ionization energy (10.18 eV) and hence one can expect higher bonding interaction with the surface. Estimated response values for ZnO NWs were 80.2, 1.6, 1.1 and 1.1 for NH_3, H_2O, $(CH_3)_2CO$ and C_2H_5OH, respectively. This experimental response was compared to the theoretical results to validate the obtained results. The response of the ZnO NWs was estimated using equation (2). The calculated values were 25.3, 76.0, 4.7 and 0 for ammonia, water, acetone and ethanol, respectively. The response of the H_2O adsorption system was found to be high. Nevertheless, experimentally, the deposited ZnO NWs showed a good

response towards NH_3. This might be due to the aspect ratio, porosity and charge transfer in the NW network. In reality, there will be plenty of vapour molecules that interact over the entire sensing element surface. However, a large number of closely adsorbed molecules may lead to repulsion due to steric effect [14]. It is difficult to discuss this steric effect with the chosen computational methods. Hence, there is a significant difference between experimental and computationally obtained response values.

4. Conclusion

Adsorptions of NH_3, H_2O, $(CH_3)_2CO$ and C_2H_5OH over ZnO NWs were observed through theoretical and experimental studies. For experimental analysis, vertically aligned ZnO NWs with the aspect ratio of 34 were deposited on a glass substrate by the SILAR method. Theoretical studies reveal that the ZnO NW has a high response to water molecules and its response value is 76. However, in reality, the ZnO NWs show a better response (80.2) towards NH_3 vapour than all the other vapours. This difference arises due to the lack of dispersion interactions and a single molecule used in computational studies. The charge transfer from NH_3 to ZnO was $0.02|e|$ and binding energy was 14.6 eV. The ZnO NWs band gap decreased from 0.34 to 0.26 eV and Zn 3d band was altered after NH_3 adsorption. The observed results reveal that the ZnO NWs is a promising material for detecting ammonia.

Acknowledgements

This study was funded by Defence Research and Development Organisation (DRDO), India, under ER & IPR Project (ERIPR/ER/1003908/M/01/1541). We thank Dr Arkaprava Bhattacharyya, SASTRA University, for providing ATK QuantumWise software to carry out the DFT studies. We also thank SASTRA University for providing the infrastructural facility to carry out the research work.

References

[1] Lexi Z, Jianghong Z, Haiqiang L, Liming G, Li L, Jianfeng Z *et al* 2011 *Sens. Actuators B* **160** 364
[2] Mohini D, Jitendra B, Ashok S, Vimal V and Golla E 2014 *IEEE Sens. J.* **14** 1577
[3] Samarasekara P, Yapa N U S, Kumara N T R N and Perera M V K 2007 *Bull. Mater. Sci.* **30** 113
[4] Shudi P, Gaolin W, Wei S and Qian W 2013 *J. Nanomater.* **2013** 1
[5] Rajesh K, Al-Dossary O, Girish K and Ahmad U 2015 *Nano-Micro Lett.* **7** 97
[6] Kalyamwar V S, Raghuwanshi F C, Narayan L J and Anil J G 2013 *J. Sens. Technol.* **3** 31
[7] Akash K, Sun-Woo C, Hyoun W K and Sang S K 2015 *J. Hazard. Mater.* **286** 229
[8] Wagh M S, Jain G H, Patil D R, Patil S A and Patil L A 2006 *Sens. Actuators B* **115** 128
[9] Bhooloka Rao B 2000 *Mater. Chem. Phys.* **64** 62
[10] Hsueh H T, Hsueh T J, Chang S J, Hung F Y, Hsu C L, Dai B T *et al* 2012 *IEEE Trans. Nanotechnol.* **11** 520
[11] Martins J B L, Longo E, Salmon O D R, Espinoza V A A and Taft C A 2004 *Chem. Phys. Lett.* **400** 481
[12] Prades J D, Cirera A and Morante J R 2009 *Sens. Actuators B* **142** 179
[13] Meyer B and Marx D 2003 *J. Phys.: Condens. Matter* **15** 89
[14] Noei H, Gallino F, Jin L, Zhao J, Valentin C D and Wang Y 2013 *Angew. Chem. Int. Ed.* **52** 1977
[15] Morimoto T, Yanal H and Nagao M 1976 *J. Phys. Chem.* **80** 471
[16] Ozawa K, Hasegawa T, Edamoto K, Takahashi K and Kamada M 2002 *J. Phys. Chem. B* **106** 9380
[17] Yuan Q, Zhao Y P, Li L and Wang T 2009 *J. Phys. Chem. C* **113** 6107
[18] Virtual Nanolab version 2016.0 QuantumWise A/S (www.quantumwise.com)
[19] Brandbyge M, Mozos J L, Ordejon P, Taylor J and Stokbro K 2002 *Phys. Rev. B* **65** 165401
[20] Soler J M, Artacho E, Gale J D, García A, Junquera J, Ordejón P *et al* 2002 *J. Phys.: Condens. Matter* **14** 2745
[21] Perdew J P, Burke K and Ernzerhof M 1996 *Phys. Rev. Lett.* **77** 3865
[22] Mulliken R S 1955 *J. Chem. Phys.* **23** 1833
[23] Amalraj A S and Senguttuvan G 2014 *J. Mater. Sci.: Mater. Electron.* **25** 2035
[24] Pandeeswari R and Jeyaprakash B G 2014 *Sens. Actuators B* **195** 206
[25] Mohammadi A S, Mahdy Baizaee S and Salehi H 2011 *World Appl. Sci. J.* **14** 1530
[26] Charifi Z, Baaziz H and Reshak A H 2007 *Phys. Stat. Sol. (b)* **244** 3154
[27] Agapito L A, Curtarolo S and Nardelli M B 2015 *Phys. Rev. X* **5** 011006
[28] Arockia J K, Jonnala R R, Parthasarathy S, Babu K J, Ganesh K M, Prabakaran S *et al* 2016 *J. Alloys Compd.* **688A** 422